Analysis of Fretting Fatigue Strength of Integral Shroud Blade for Steam Turbine

Yasutomo KANEKO*, Masayuki Tomii*, Hiroharu Ohyama**, and Takayuki Kurimura**
*Takasago Research & Laboratory Center
MITSUBISHI HEAVY INDUSTRIES, LTD.,
2-1-1 Shinhama Arai-Cho, Takasago Hyogo 676-8686, Japan
(E-mail: yasutomo_kaneko@mhi.co.jp, masayuki_tomii@mhi.co.jp)
**Takasago Machinery Works
MITSUBISHI HEAVY INDUSTRIES, LTD.,
2-1-1 Shinhama Arai-Cho, Takasago Hyogo 676-8686, Japan
(E-mail: hiroharu_ooyama@mhi.co.jp, takayuki_kurimura@mhi.co.jp)

ABSTRACT: To improve the reliability and the thermal efficiency of LP (Low Pressure) end blades of steam turbine, new standard series of LP end blades have been developed. The new LP end blades are characterized by the ISB (Integral Shroud Blade) structure. In the ISB structure, blades are continuously coupled by blade untwist due to centrifugal force when the blades rotate at high speed. One of the probable failure modes of the ISB structure seems to be fretting fatigue, because the ISB utilizes friction damping between adjacent shrouds and stubs. Therefore, in order to design a blade with high reliability, the design procedure for evaluating the fretting fatigue strength was established by the model test and the nonlinear contact analysis. This paper presents the practical design method for predicting the fretting fatigue strength of the ISB structure, and the some applications are explained.

Keywords: Blade, Vibration, Fretting fatigue, Vibratory stress, Nonlinear analysis

1 INTRODUCTION

New standard series of LP end blades of steam turbine have been developed to improve the thermal efficiency and the reliability. The new LP end blades are characterized by the ISB structure [1]. More than 15 types of LP end blades including the 3600 rpm 45 inch titanium blade and 1500/1800 rpm 54 inch blade have applied the ISB structure as shown in Fig. 1, and successfully operated in many plants. In the ISB structure, blades are continuously coupled by blade untwist due to centrifugal force when the blades rotate at high speed. Therefore, the number of the resonant vibration modes can be reduced by virtue of the vibration characteristics of the circumferentially continuous blades, and the resonant stress can be decreased due to the additional friction damping generated at shrouds and stubs.

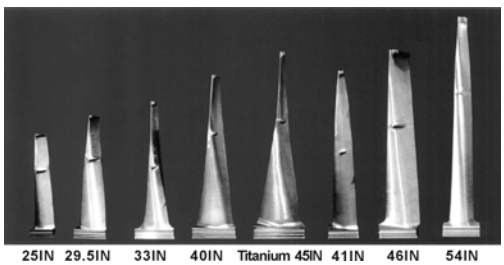

Fig.1 Series of low pressure end blade

In order to develop the new LP end blades with high reliability, analysis methods for the vibration characteristics of the ISB structure were developed and their validity was confirmed before applying them to the blade design [2, 3]. Moreover, the final reliability of the developed blades has been confirmed by verification tests such as rotational vibration tests and actual loading tests, and these test results have been accumulated into the database [4]. The accuracy of the predicted frequency and the vibratory stress has been improved, using the database of the test results.

One of the probable failure modes of the ISB structure seems to be fretting fatigue, because the ISB utilizes friction damping between adjacent shrouds and stubs. Therefore, in order to design a blade with high reliability, the design procedure for evaluating the fretting fatigue strength was established, using the results of the fretting model test and the nonlinear contact analysis.

This paper presents the practical design method for predicting the fretting fatigue strength of the ISB structure, and some applications are explained.

2 ANALYSIS OF LOCAL VIBRATORY STRESS AT CONTACT EDGE

2.1 Introduction of stick factor of shroud

In order to evaluate the fretting fatigue strength of the shroud when designing the ISB structure, it is necessary to obtain the local vibratory stress at the contact edge of the shroud by the nonlinear contact analysis including the friction effect [5]. In actual blade design, however, it is unpractical to calculate the local vibratory stress at the contact edge of the shroud every time by the nonlinear contact analysis. Therefore,

in the method presented here, the nonlinear local vibratory stress at the contact edge of the shroud is evaluated, multiplying the linear local vibratory stress by the correction factor, which considers the friction between the shrouds. In other words, this correction factor, which is called the stick factor at the shroud hereafter, is defined as Eq. (1).

$$\alpha(\theta,\phi,\mu_T)=\frac{\sigma_{n,v}}{\sigma_{l,v}} \tag{1}$$

Where, $\sigma_{n,v}$ denotes the local vibratory stress at the shroud by the nonlinear contact analysis including the friction effect, and $\sigma_{l,v}$ the local vibratory stress at the shroud by the linear analysis, in which the adjacent shrouds are assumed to be completely stuck. The angles of ϕ and θ are the shroud contact angles, and the definition of the shroud contact angle is shown in Fig. 2. μ_T is the ratio of the shroud reaction force, P and the friction force, F_T, and is called tangential force coefficient hereafter. The tangential force coefficient, μ_T is defined as Eq. (2).

$$\mu_T=\frac{F_T}{P} \tag{2}$$

The procedure for obtaining the fretting fatigue strength and the stick factor α is shown in Fig. 3.

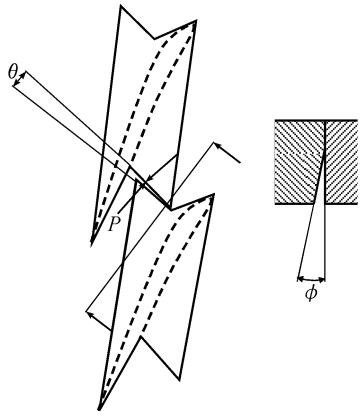

Fig.2 Definition of shroud contact angle

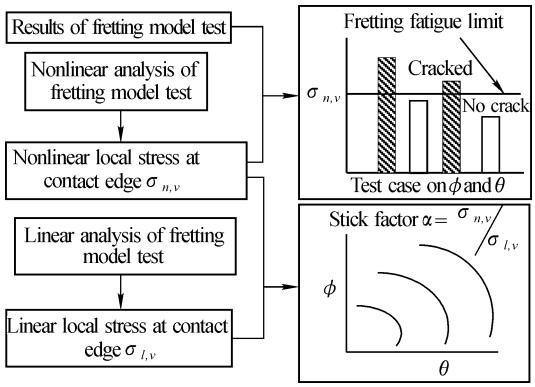

Fig.3 Procedure for obtaining fretting fatigue strength and stick factor

2.2 Analysis of linear vibratory stress

Excitation forces exerting on a steam turbine blade under operation can be classified into 3 categories.

(1) Harmonic excitation force of the lower engine order caused by the flow distortion.

(2) Stage interaction force coming from the wake of the upstream vane or the potential field of the upstream/downstream vane.

(3) Random excitation force under low load and low vacuum condition.

In order to evaluate the local vibratory stress at the contact edge of the shroud caused by these excitation forces, first, the linear response analysis is carried out, and the linear local vibratory stress, $\sigma_{l,v}$ is calculated. Next, multiplying the linear local vibratory stress, $\sigma_{l,v}$ by stick factor α, the local nonlinear vibratory stress $\sigma_{n,v}$ is obtained according to Eq. (1). The detailed procedure to obtain the local nonlinear vibratory stress $\sigma_{n,v}$ is as follows.

(1) Calculate the shroud reaction force, P and the contact region of the shroud by the nonlinear contact analysis (static analysis for centrifugal force) at the rated speed, which considers the effect of the large deformation of the blade and the friction between the shrouds.

(2) Carry out the linear response analysis of the bladed disk by use of the cyclic symmetry method to obtain the linear local vibratory stress, $\sigma_{l,v}$ caused by the harmonic excitation force, stage interaction force and so on. In the linear response analysis, the cyclic symmetry condition is applied to the only contact region of the shroud calculated by the nonlinear contact analysis.

(3) Obtain the tangential force coefficient μ_T from the shroud reaction force, P calculated by the nonlinear contact analysis, and the friction force F_T calculated by the linear response analysis.

(4) Obtain the actual local vibratory stress $\sigma_{n,v}$ at the contact edge of the shroud, multiplying the linear local vibratory stress, $\sigma_{l,v}$ calculated by the linear analysis by the stick factor α. The stick factor α, is determined from the shroud contact angle ϕ and θ calculated by the nonlinear contact analysis, and the tangential force coefficient μ_T above.

The detailed procedure to calculate the linear vibratory stress is describes below.

2.3 Analysis of resonant stress by modal analysis method

When the bladed disk system of the ISB structure is rotating in the circumferentially non-uniform flow, the equation of motion for the bladed disk system shown in Fig. 4, can be expressed by Eq. (3).

$$[M_T]\{\ddot{U}_T\}+[C_T]\{\dot{U}_T\}+[K_T]\{U_T\}=\{P_T\} \tag{3}$$

Where, $[M_T]$, $[C_T]$, $[K_T]$,$\{U_T\}$, and $\{P_T\}$ are the mass matrix, damping matrix, stiffness matrix, displacement vector and

excitation force vector of the whole bladed disk system.

Although the detailed procedure to obtain the solution of Eq. (3) is not written here for lack of space, applying the cyclic symmetry method and the modal analysis method, and introducing the modal damping to Eq. (3), the resonant stress of the blade to the excitation force of engine order H can be expressed by Eq. (4) and Eq. (5) [6].

$$\{\sigma_k\}=\frac{1}{2\varsigma_m}\frac{1}{M_m\omega_m^2}\left[\{A_\sigma\}\cos(\omega t-k\alpha_H)+\{B_\sigma\}\sin(\omega t-k\alpha_H)\right] \quad (4)$$

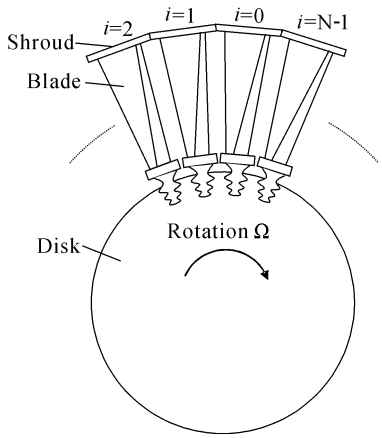

Fig.4 Bladed disk system of ISB

$$\left.\begin{aligned}\{A_\sigma\}&=\left\{\phi_I^m\right\}^T\{P\}\left\{\sigma_R^m\right\}-\left\{\phi_R^m\right\}^T\{P\}\left\{\sigma_I^m\right\}\\ \{B_\sigma\}&=\left\{\phi_I^m\right\}^T\{P\}\left\{\sigma_I^m\right\}+\left\{\phi_R^m\right\}^T\{P\}\left\{\sigma_R^m\right\}\end{aligned}\right\} \quad (5)$$

Where, M_m, ς_m and ω_m are the modal mass, modal damping ratio, and natural angular frequency of the m-th vibration mode. The vector $\{\sigma_k\}$ is the vibratory stress of the k-th blade. The vector $\{\phi_R^m\}$ and $\{\phi_I^m\}$ are the real and imaginary mode of a blade, respectively, while $\{\sigma_R^m\}$ and $\{\sigma_I^m\}$ are the vibratory stress modes corresponding to the vector $\{\phi_R^m\}$ and $\{\phi_I^m\}$. The vector $\{P\}$ is the amplitude of the excitation force acting on a blade, ω the angular frequency, and α_H the inter-blade phase angle caused by the rotation of the bladed disk system.

2.4 Resonant stress caused by excitation force of lower engine order

Using the modal information obtained from 3D FEA, the resonant stress of the ISB can be calculated by Eq. (4), if the excitation force, $\{P\}$ and the modal damping ratio, ς_m are estimated in advance. Although the recent technology has made it possible to predict the blade damping analytically, the blade damping predicted from the test results for the similar blades is more accurate. Therefore, as for the blade damping, the database, which has been prepared by accumulating the results of the actual loading tests for similar blades, is utilized. On the other hand, even a latest CFD technology cannot predict the excitation force of the lower engine order due to the flow distortion caused by the asymmetry of the case, etc. Therefore, the database is also utilized in predicting the excitation force of the lower engine order. In developing a new blade, the resonant stress is predicted as shown in Fig.5, assuming that the distribution pattern of the excitation force on a blade is the same as that of the steady gas force and the magnitude of the excitation force is proportional to that of the steady gas force. The detailed procedure is as follows.

(1) Using Eq. (4) and Eq. (6), the resonant stress of the existing blades for which the actual loading test was done is calculated as σ_{cal}.

$$\{P\}=\left\{P_{\text{steady}}\right\},\quad \varsigma_{\text{m}}=\varsigma_{\text{cal}} \quad (6)$$

Where, $\left\{P_{\text{steady}}\right\}$ is steady gas force, which can be calculated from steady CFD analysis. ς_{cal} is a proper damping ratio, and the design value or empirical value can be used for ς_{cal}.

(2) Using the resonant stress, σ_{measure} and the damping ratio, $\varsigma_{\text{measure}}$ measured by the actual loading test, stimulus (the ratio of the excitation force to the steady gas force) is calculated for each harmonic according to Eq. (7).

$$S_{\text{measure}}=\frac{\sigma_{\text{measure}}}{\sigma_{\text{cal}}}\frac{\varsigma_{\text{measure}}}{\varsigma_{\text{cal}}} \quad (7)$$

(3) Accumulating S_{measure} and $\varsigma_{\text{measure}}$ of existing blades, the database of the stimulus and the damping ratio, $\left\{S_{\text{db}}\ \varsigma_{\text{db}}\right\}$ is prepared. For a newly developed blade, the resonant stress can be predicted by Eq. (8).

$$\{P\}=S_{\text{db}}\left\{P_{\text{steady}}\right\},\quad \varsigma_{\text{m}}=\varsigma_{\text{db}} \quad (8)$$

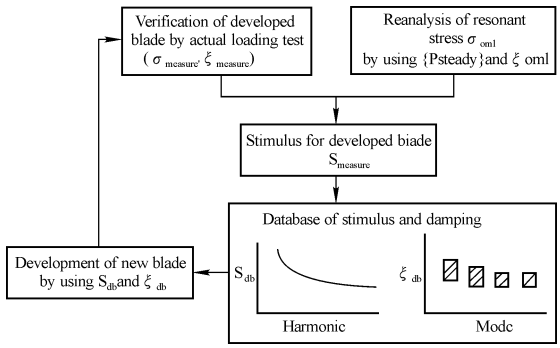

Fig.5 Procedure of predicting resonant stress for excitation force of lower engine order

2.5 Resonant stress caused by stage interaction force

In calculating the resonant response of a blade due to the nozzle wake excitation force, 3D CFD and 3D FEA are used. Fig.6 shows the procedure for calculating the resonant stress of the blade. This method is the almost same one as many published papers adopted [7, 8], and the resonant stress is calculated as follows.

(1) The pressure fluctuation on the blade surface is obtained in the form of time-history wave by the blade-vane interaction analysis with unsteady 3D CFD. The magnitude and the phase of the pressure fluctuation with the fundamental frequency (the rotor speed multiplied by the vane count) are calculated by Fourier analysis.

(2) The eigenvalue analysis of the bladed disk is carried out by 3D FEA, and the resonant stress is calculated by Eq. (4). The magnitude and the phase of the excitation force on each grid point of FE model are obtained by the pressure fluctuation

calculated by 3D CFD, multiplying the pressure fluctuation by the effective area around the grid point. The calculated value or empirical value is used for the blade damping.

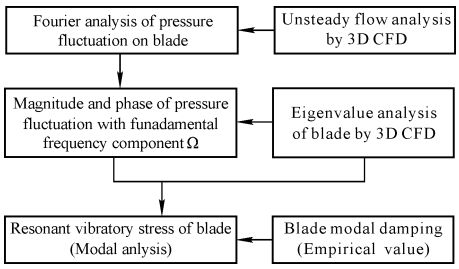

Fig. 6 Procedure for calculating resonant caused by stage interaction force

2.6 Vibratory stress caused by random excitation force

Vibratory stress caused by random excitation force under low load and low vacuum condition may be predicted analytically if the random excitation force is known. However, it is very difficult to predict the random excitation force on a blade caused by inverse flow, flow separation, and so on. Therefore, the random excitation force is predicted by use of the database of the actual loading test as well as the excitation force of the lower engine order. In the actual loading test, the operation condition of the turbine load and the condenser vacuum was widely changed, and the random vibratory stress of the tested blade was measured with a strain gauge. The measured random vibratory stress was normalized as Eq. (9) by use of the modal stiffness and the modal damping of the blade, and so on. Finally, the normalized random vibratory stress, A_{random} has been accumulated into the database.

$$A_{random} = \frac{\sigma_{measure}}{\left(\frac{1}{2\varsigma_m}\frac{s_e A_e p_e}{M_m \omega_m^2}\right)_{measure} \sigma_{rel}} \tag{9}$$

Where, σ_{rel} is the relative stress of the gauge location calculated by FEA, A_e the effective blade area receiving the random excitation force, p_e the reference pressure, and s_e the empirical factor representing the effect of the diffuser geometry and so on. The subscript "*measure*" refers to the measured blade. The random vibratory stress of a newly developed blade (the linear vibratory stress, $\sigma_{l,v}$) can be predicted by Eq. (10)

$$\sigma_{l,v} = A_{random}\left(\frac{1}{2\varsigma_m}\frac{s_e A_e p_e}{M_m \omega_m^2}\right)_{new} \sigma_{rel,sh} \tag{10}$$

Where, $\sigma_{rel,sh}$ is the local vibratory stress at the contact edge of the shroud calculated by the FEA, and the subscript "*new*" refers to the newly developed blade.

3 RESULTS OF ANALYSIS AND MEASUREMENT

3.1 Stick factor of shroud

The fretting model test was carried out under the loading cycles of 10^7 times by use of the model shroud, and the condition of the incidence of the fretting crack was examined by changing the shroud contact angle ϕ and θ. In the fretting model test, the shroud reaction force was adjusted so that the average contact pressure was around the design value. The relative slip between shrouds was adjusted so as to be an expected value of an actual turbine blade.

The commercial FE package code ANSYS was used to calculate the nonlinear local stress at the contact edge of the model shroud, where the maximum tangential stress in the contact plane around the contact region was defined as the local stress at the contact edge of the shroud. In the analysis, first, the optimal mesh for the nonlinear analysis was selected by the parametric study on mesh size, where the convergence of the solution was examined, and the comparison between the calculated and measured stress was made. The optimal FEA mesh was determined from the results of the parametric study, and in all the analyses of the fretting fatigue strength of the shroud, the same FEA mesh was used. From the results of the nonlinear analysis of the fretting model test, it was found that the incidence of the fretting fatigue cracks can be discriminated by use of the local contact stress at the contact edge calculated by the nonlinear contact analysis including the friction effect.

Next, the results of the fretting model test were re-analyzed by the linear analysis, and the stick factor of the shroud was obtained by Eq. (1). Fig.7 shows an example of the stick factor of the shroud. In the linear analysis, the contact region, which was determined by the nonlinear contact analysis in advance, was assumed to be completely stuck, and no slips between shrouds occur. As shown in Fig.7, the larger the shroud contact angle ϕ and θ are, the larger the stick factor of the shroud is. This result shows that when the shroud contact angle ϕ and θ become large, the reduction effect on the local stress due to slip decreases, and the local stress at the contact edge increases. This is the reason why the fretting fatigue crack is easy to occur when the adjacent shrouds partially get contact with each other.

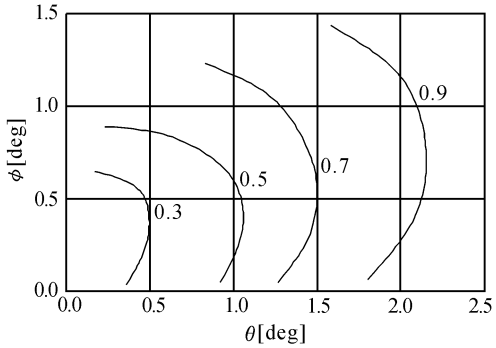

Fig.7 Example of slip factor of shroud (μ_T= 0.5)

3.2 Calculated and measured blade deformation due to centrifugal force

For the ISB structure, a mechanical clearance exists between the shrouds at standstill. With increasing rotational speed of the turbine, the clearance reduces and the shroud connection is coupled above a certain speed. The static and dynamic local stresses at the contact edge of the shroud depend significantly on its real contact condition.

In the analysis of the blade deformation due to centrifugal force, the contact area, the contact stress distribution, etc. at the rated speed were evaluated by simulating the blade deformation from the standstill to the rated speed condition by the nonlinear contact analysis. The commercial FE package code ANSYS was applied for the nonlinear contact analysis, and the friction coefficient between shrouds and stubs was assumed to be 0.5 based on the results of fretting model tests.

Fig.8 shows the typical FE model of a low pressure end blade of a fossil steam turbine used in the deformation analysis due to centrifugal force. In order to predict the real contact condition of the shroud and stub, the fine mesh was applied to the contact surface of the shroud and stub. The fine mesh of the shroud and stub in Fig.8 was determined by the parametric study on the mesh size for the fretting model test.

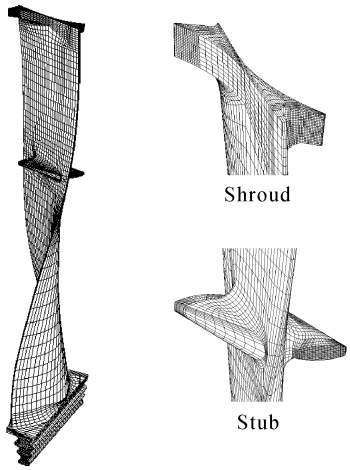

Fig.8 Typical FE model of fossil turbine blade

In order to verify the validity of the analysis of blade deformation due to centrifugal force, the blade deformation in rotation was measured and compared with the calculated one. In the measurement of the blade deformation, the stroboscope and the CCD camera were used to take the instant picture of the blade in rotation. Then, the blade deformation was calculated as the difference between the blade positions of the rotating and the standstill condition. Fig.9 shows the measurement system of blade deformation in rotation. Fig.10 shows the comparison of the measured and the calculated blade deformation, and the calculated result shows good agreement with the measured one. From these results, it can be said that the blade deformation caused by centrifugal force can be correctly predicted by the nonlinear contact analysis adopted here. Although the local vibratory stress of the contact edge at the shroud was not measured directly, it seems that the nonlinear contact analysis can predict it with practical accuracy because the blade deformation, which determines the boundary condition of the dynamic analysis, was predicted correctly.

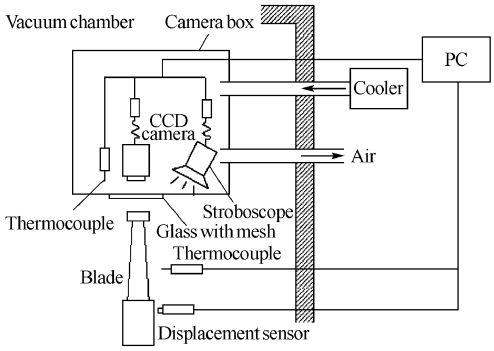

Fig.9 Measurement system of blade deformation

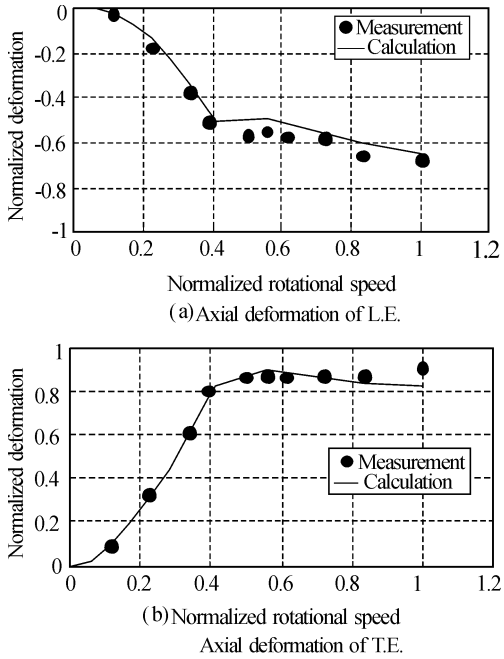

Fig.10 Comparison of measured and calculated shroud deformation due to centrifugal force

3.3 Calculated and measured vibration characteristics

In the ISB structure, the blade is brought into contact with the adjacent blade at the shroud and the stub. Because the ISB structure is cyclically symmetric and shows the vibration characteristics of the continuous ring type structure, in the vibration analysis only one blade is modeled and the eigenvalue analysis of Eq. (3) is first carried out by use of the cyclic symmetry method. When evaluating the fretting fatigue strength of the ISB structure, the cyclic condition, under which the shrouds and stubs are continuously coupled, is applied to the only real contact region of the shrouds and stubs calculated by the nonlinear contact analysis in advance. After the linear vibratory stress is calculated from Eq. (4) and Eq. (10) using the modal information obtained from the eigenvalue analysis, the real local vibratory stress at the contact edge of the shroud is calculated from Eq. (1).

Fig.11 shows the comparison of the natural frequencies of the bladed disk of a fossil steam turbine for different cyclic conditions. In the partial contact case in Fig.11, the cyclic condition is applied to the only upper contact region of the shroud. On the other hand, in the full contact case in Fig.11, the cyclic condition is applied to the whole contact surface of the shroud. As for the stub, the cyclic condition is applied to the whole contact surface for both cases. In Fig.11, natural frequencies measured in the rotational vibration test are also plotted. Fig.12 shows the comparison of the local vibratory stress at the contact edge of the shroud for the real and full contact case. The comparison of the vibratory stress of the blade profile is made in Fig.13. From these results, it can be said that the cyclic condition of the shroud has little effect on the natural frequency and the vibratory stress of the blade profile, but is very sensitive to the local vibratory stress at the contact edge of the shroud. It is also observed in the fretting model test that the local vibratory stress at the contact edge of the shroud is sensitive to the shroud contact condition (the shroud contact angles of ϕ and θ). From these results, it is concluded that it is indispensable to correctly predict the shroud contact condition for evaluating the fretting fatigue strength of the shroud.

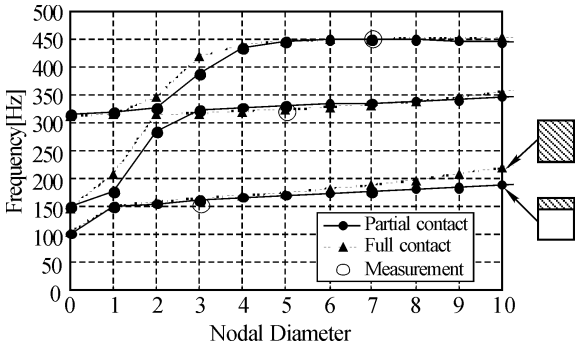

Fig. 11 Natural frequency of fossil turbine blade for different cyclic conditions

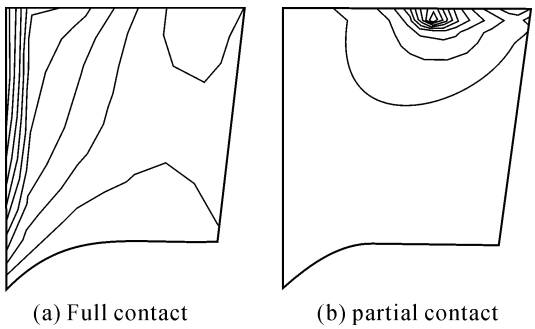

Fig.12 Local vibratory stress of shroud for different cyclic conditions

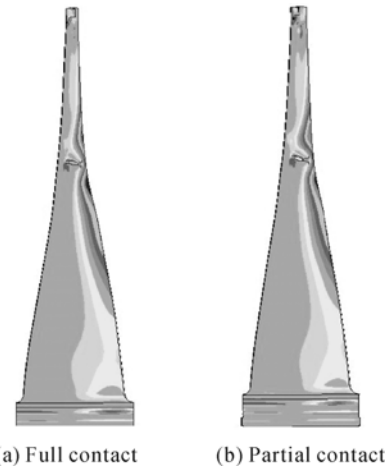

Fig.13 Vibratory stress of blade profile for different cyclic conditions (Principal stress of 1st mode with 3 nodal diameter)

3.4 Evaluation of fretting fatigue strength

In the design of the ISB structure of a low pressure steam turbine, the fretting fatigue strength can be evaluated according to the procedure described in the above section. Fig.14 shows the fretting fatigue strength of a nuclear turbine blade. In evaluating the fretting fatigue strength, first, the resonant stress and the random vibratory stress caused by probable excitation forces were calculated. Second, the real vibratory stress at the contact edge of the shroud was calculated from Eq. (1), and the fretting fatigue strength was evaluated, comparing the allowable stress obtained from the results of fretting model test. From these results, it can be said that this blade has the sufficient fretting fatigue strength against the all kinds of vibratory stresses.

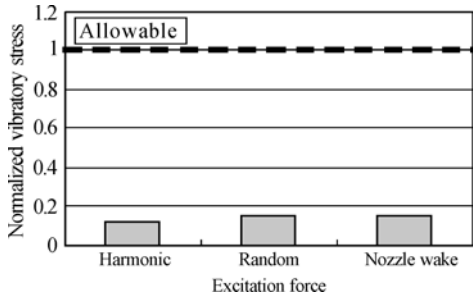

Fig.14 Fretting fatigue strength of fossil turbine blade

Fig.15 shows the comparison of the fretting fatigue strength of a fossil turbine blade with the different shroud taper angles. In the case of optimal contact, in order to increase the fretting fatigue strength, the shroud taper angle is adjusted so that the shroud contact angles of ϕ and θ are nearly zero (surface contact condition) by making the shroud taper angle opposite to the contact angles calculated by the nonlinear analysis. For both of the original and the optimal contact case, the local vibratory stress at the contact edge of the shroud caused by the

excitation force of the lower engine order is calculated, and the fretting fatigue strength is compared. From these results, it can be said that the fretting fatigue strength can be remarkably increased by setting the shroud taper angle opposite to those calculated by nonlinear centrifugal force analysis.

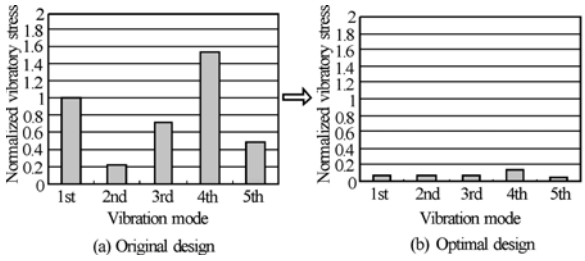

Fig.15 Fretting fatigue strength of fossil turbine blade with different shroud taper angle

4 CONCLUSION

This paper, first, presents the procedure for evaluating the fretting fatigue strength of the ISB structure of a low pressure steam turbine. Second, the result of the fretting model test is re-analyzed to confirm the correlation between the calculated local stress and the incidence of the crack at the contact edge of the shroud. The shroud deformation due to centrifugal force is also measured in order to confirm the accuracy of the nonlinear contact analysis. From these results, it is shown that the fretting fatigue strength of the ISB structure can be evaluated with practical accuracy.

The example of the evaluation of the fretting fatigue strength of the actual blade is illustrated, and it is shown that the fretting fatigue strength can be increased by setting the shroud taper angle opposite to the calculated contact angle.

The ISB structure developed by these technologies has been successfully operating in the field since the first application. Hereafter, the ISB structure will be applied not only for new turbines but also for any existing turbine refurbishment to improve the efficiency and the reliability.

REFERENCES

[1] Watanabe, E., Ohyama, H., Kaneko, Y. and Miyawaki, T., "Development of New Advanced Low Pressure End Blades for High Efficiency Steam Turbine," *JSME International Journal*, Series B, Vol. 45, No. 3, pp.552-558, 2002.

[2] Kaneko, Y. and Mase, M., and Watanabe, E., "Vibration Analysis of Integral Shroud Blade for Steam Turbine," *Proceeding of International Conference on Power Engineering*-97 (ICOPE-97), Tokyo, pp.455-460, 1997.

[3] Kaneko, Y., Mori, K. and Ohyama, H., "Measurement and Analysis of Random Vibration of steam Turbine Low Pressure End Blade," IFToMM, Proceedings of Sixth International Conference on Rotor Dynamics, Vol. 3, pp. 153-159, 2002.

[4] Kaneko, Y., Mori, K., and Ohyama, H., "Development and Verification of 3000 rpm 48 inch Integral Shroud Blade for Steam Turbine," Proceedings of the ASME Power Conference 2005, PWR2005-50347, pp.609-616, 2005.

[5] Kondo, Y., and Bodai, M., "Study on Fretting Fatigue Crack Initiation Mechanism Based on Local Stress at Contact Edge (in Japanese)," Transaction of the Japan Society of Mechanical Engineering, Series A, Vol. 63, No. 608, pp.669-676, 1997.

[6] Kaneko, Y., Mori, K., and Tochitani, N., "Analysis and Measurement of Resonant Vibratory Stress of Integral Shroud Blade for Steam Turbine," Proceedings of the International Conference on Power Engineering-03 (ICOPE-03), Vol.2, pp.189-194, 2003.

[7] Chiang, H. D. and Kielb, R. E., "An analysis system for blade forced response, " *Journal of Turbomachinery*, vol. 115, pp.762-770, 1993.

[8] Hilbert, G. R., Ni, R. H. and Takahashi, R. K., "Forced response prediction of gas turbine rotor blades," ASME Winter Annual Meeting, 1997.